Simple Scheme To Evaluate Crystal Nonlinear Susceptibilities: Semiempirical AM1 Model Investigation of 3-Methyl-4-nitroaniline Crystal

Frédéric Castet* and Benoît Champagne†

Laboratoire de Chimie Théorique Appliquée, Facultés Universitaires Notre-Dame de la Paix, 61 rue de Bruxelles, B-5000 Namur, Belgium

Received: October 12, 2000

A simple multiplicative scheme is proposed for the evaluation of the second-order nonlinear susceptibility of molecular crystals from the knowledge of the first hyperpolarizability of small molecular clusters. The principle of this new scheme is illustrated at the semiempirical AM1 level for 3-methyl-4-nitroaniline crystal.

I. Introduction

Because of their large nonlinear optical (NLO) responses, molecular crystals based on conjugated organic chromophores are attractive materials for technological applications such as electrooptical modulators and frequency mixers. To fabricate the most efficient NLO devices, an interdisciplinary design combines (i) the synthesis of new chromophores, (ii) their physicochemical characterizations, (iii) crystal engineering, and (iv) quantum chemical investigations. The latter encompass the determination of the NLO responses, the deduction of structure−property relationships, and the physical description of the molecular NLO phenomena.[1−4] At the microscopic level, the NLO responses are characterized by the first (β) and second (γ) hyperpolarizabilities while the second- ($\chi^{(2)}$) and third-order ($\chi^{(3)}$) nonlinear susceptibilities describe their macroscopic analogues, respectively. Although molecular interactions in the solid state can have a major role on the macroscopic NLO properties, most of the theoretical investigations have been limited to the determination of the microscopic molecular NLO responses. The first model relating the microscopic to the macroscopic NLO responses was the oriented gas approximation introduced by Chemla et al.[5] It relies on two approximations: (i) the molecular hyperpolarizabilities are assumed to be additive, i.e., the crystal susceptibilities are obtained by performing the tensor sum of the hyperpolarizabilities of the unit cell molecules, and (ii) the effects of the molecular surrounding are approximated using local field factor corrections.

This approximation was used by Zyss and Oudar[6] to investigate how the crystal point group influences the relation between the microscopic and macroscopic second-order NLO responses and which orientation of the chromophores in the unit cell leads to the highest phase-matching, maximizing therefore the crystal optical nonlinearity. At the same time, improvement of the oriented gas approximation was achieved in a study about the crystal of urea due to Zyss and Berthier.[7] To account for the surrounding effects including the intermolecular hydrogen bonding, point charges have been distributed around the molecules. As noted by these authors, further improvements should consist of replacing the point-charge potential by the full-multipolar-molecular wave function potential as well as in including exchange, dispersion, and intermolecular charge transfer contributions. Some of these effects are described by the so-called polarizable continuum model (PCM), originally elaborated to describe solute−solvent interactions, and of which the extensions include the treatment of anisotropic and ionic media as well as of the Pauli repulsion and dispersion terms.[8−9] Several studies have adopted this scheme to determine the NLO properties of molecules in solution[10−13] but, to our knowledge, it has not yet been used for molecular crystals.

An alternative approach is the full treatment of the 3D periodic crystals with the tools of band structure theory but, although progresses toward these directions have recently been achieved, applications to nonlinear responses remain scarce.[14−16] On the other hand, besides its computational limitations, the supermolecule approach where the crystal is modeled by a molecular cluster constitutes the straightforward method to include these nonadditive intermolecular effects. This approach has been used to elucidate the relations between the relative orientation of molecular packing of small clusters of *p*-nitroaniline[17,18] and their second-order NLO response. In addition to assess the limitations of the oriented gas approximation, the ZINDO study of Di Bella et al.[18] demonstrated that the dominant component of β is maximized for a stacked pair of *p*-nitroaniline molecules when they are in a slipped cofacial arrangement such that the donor of one molecule is directly above the acceptor of the other. On the other hand, other packing structures (stacked dimers including the situation where their dipolar axes are rotated with respect to one another) lead to a decrease of the first hyperpolarizability with respect to the value for the isolated molecule.[17−18] Due to their 3D nature, different orientations of intermolecular interactions occur in crystals and it is therefore important to average over these various orientations in order to determine the bulk nonlinear response. This 3D nature of the crystal packing is considered here for the determination of the electronic second-order susceptibility of MNA (3-methyl-4-nitroaniline) crystal. We first determine the crystal packing effects upon β along each crystallographic axis. Then, we estimate the crystal nonlinear susceptibility by adopting a simple multiplicative scheme of which the validity is addressed. The MNA crystal can be considered as a prototype for investigating the bulk second-order NLO responses because it possesses the chemical simplicity of *p*-nitroaniline whereas the presence of the methyl group ensures a noncentrosymmetric crystal packing. The studies of Yasukawa et al.[17] and Di Bella et al.[18] have been carried out at a semiempirical level for obvious

* Corresponding author. Present address: Laboratoire de Physico-Chimie Moléculaire, UMR 5803 CNRS, 351 Cours de la Libération, 33405 Talence Cedex, France.

† Research associate of the Belgian National Fund for Scientific Research.

10.1021/jp003746s CCC: $20.00
Published on Web 02/07/2001

reasons. This is also the strategy we adopt in this work. In particular we have chosen the AM1 (Austin model 1)[19] Hamiltonian and have checked its performance against ab initio Hartree−Fock and post Hartree−Fock calculations on small clusters.

It is of importance to note that, to alleviate the size difficulties, several electrostatic models have also been elaborated[20−22] where the intermolecular interactions are represented by classical electrical interactions between distributed multipoles and (hyper)polarizabilities. References 23 and 24 are typical examples that illustrate the classical electrostatic interaction treatment for second- and third-order NLO compounds. The work of Hamada[25] on MNA molecular pairs shows that the simple electrostatic treatment, where the molecules are modeled by point dipoles located at the center of mass, reproduces fairly well the first hyperpolarizability obtained within the supermolecular approach. Moreover, it defines the limitations of the oriented gas approximation. Later, Hamada[26] shows that the oriented gas approximation can be improved by using experimental refractive indices for the local field factors. In this sense our study can be viewed as a continuation of the work of Hamada. It concentrates on the description of the crystal packing effects upon the static electronic first hyperpolarizability of MNA and on the elaboration of a simple scheme to determine the crystal nonlinear susceptibility. Frequency dispersion and vibrational contributions are left for future investigations. The work is organized as follows: Section II describes the methodological tools and the computational procedure; the crystal and molecular structures are given in section III. Section IV presents and discusses the results before we conclude in section V.

II. Theoretical Background

The components of the static electronic first hyperpolarizability tensor of molecular clusters have been evaluated at the RHF/AM1 level by using the finite field (FF) technique[27] implemented in the semiempirical electronic structure program AMPAC[28] according to Kurtz et al.[29] It consists of computing the field-dependent total electronic energy, $E(\mathbf{F})$, for an ensemble of external electric fields, $\mathbf{F} = (F_x, F_y, F_z)$, of different amplitudes and directions and of differentiating it numerically to get the properties,

$$E(\boldsymbol{F}) = E(0) - \mu_i F_i - \frac{1}{2!}\alpha_{ij}F_iF_j - \frac{1}{3!}\beta_{ijk}F_iF_jF_k - \frac{1}{4!}\gamma_{ijkl}F_iF_jF_kF_l - \ldots \quad (1)$$

where summations over the repeated indices are assumed, $E(0)$ is the energy without electric field, μ_i is the dipole moment component along the Cartesian axis $i = x, y, z$. In Kurtz et al. FF procedure,[29] the components of the (hyper)polarizability tensors (α_{ij}, β_{ijk}, and γ_{ijkl}) are obtained by truncating eq 1 to fourth order and by using as many field amplitudes as unknown in eq 1; i.e. four (six) field amplitudes for diagonal (off-diagonal) elements of β. Field amplitudes of 0.001 au and 0.002 au have been chosen to achieve an accuracy of 1.0 au or better on β. This choice results from a compromise between two opposite effects: too large external fields would invalidate the truncation of eq 1 to fourth order, whereas too small fields would reduce the number of significant digits on the derivatives. The use of the analogue of eq 1 for the dipole moment has further confirmed the numerical accuracy of the numerical FF procedure because, for variational wave functions as those obtained at the RHF/AM1 level, the expansion coefficients of the field-dependent dipole moment and energy are identical. This FF/AM1 approach provides coupled Hartree−Fock (CHF) or fully relaxed SCF (hyper)polarizabilities; i.e., the field-induced electron reorganizational effects upon the average electron−electron interactions are included. Identical (hyper)polarizability values can be obtained analytically by adopting the coupled-perturbed Hartree−Fock (CPHF) approach,[30] which determines order by order the response of the density matrix to the external electric field.

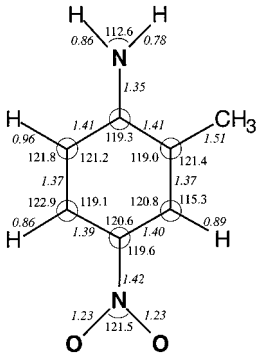

Figure 1. Bond lengths (Å) and angles (degrees) of the MNA molecule. The hydrogen atoms linked to the benzene group are located in the plane of the ring. The dihedral angle between the benzene ring and the oxygen (hydrogen) atoms of the nitro (amine) group is 1.1° (7.2°).

In testing the adequacy of the semiempirical AM1 Hamiltonian against ab initio procedures, we have computed CHF β values for MNA and its dimers by using the CPHF procedure implemented in Gaussian98[31] with different atomic basis sets. Among the latter, the split valence 6-31G basis set[32] as well as basis sets including polarization (6-31G**[33]), diffuse (6-31++G[34]), and diffuse polarization (6-31G+D[35]) functions. Adopting eq 1 correlated β values have also been calculated at the second-order Møller−Plesset (MP2) level of approximation. The field-dependent MP2 energies have been determined using Gaussian98[31] in combination with an iterative Romberg procedure[36] to improve the accuracy on the numerical derivatives. Comparison of the semiempirical values with the CPHF and FF/MP2 ab initio data will also enable to estimate the amount of electron correlation implicitly included in the AM1 Hamiltonian.

For a given MNA cluster, the magnitude of the crystal packing effect on β is characterized by the R^{cluster} ratio defined as

$$R^{\text{cluster}} = \frac{\beta^{\text{cluster}}}{N\beta^{\text{unit}}} \quad (2)$$

where the cluster contains N units. The most logical definition of the "unit" is a stacked dimer of MNA which corresponds to halve the translational unit cell (see also section III).

III. Molecular Geometry and Crystal Structure

The geometrical structure of the MNA molecule (Figure 1) and the MNA crystal structure (Figure 2) have been taken from ref 37 of which Figures 4 and 5 describe the arrangement of the molecules in the unit cell and their alignment along the c axis, respectively. The unit cell contains four MNA molecules in a volume of 722 Å^3. From ref 37, it is clear that the molecular planes are practically perpendicular to the c axis. In the absence of detailed crystallographic data, the rotation angle between the longitudinal axis of the MNA molecule and the a axis has been taken equal to 16°. This corresponds to a minimum in the AM1

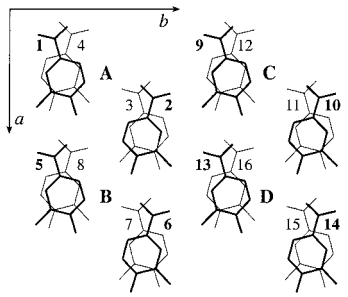

Figure 2. MNA crystal structure (hydrogen atoms are hidden for clarity) according to ref 27. *a*−*c* refer to the crystallographic axes. Bold molecules lie above the plane of the paper. The unit cell A contains the four molecules 1−4, and an equivalent numerotation is used for the unit cells B−D.

TABLE 1: Components of the AM1 Static Electronic First Hyperpolarizability Tensor (in au; 1 au = 3.206 × 10^{-53} C^3 m^3 J^{-2} = 8.641 × 10^{-33} esu) of the (1) Monomer, the (1,4) Stacked Dimer, and the (1,2,3,4) MNA Unit Cell in the Crystal Frame[a]

	β_{aaa}	β_{abb}	β_{acc}	β_{bbb}	β_{baa}	β_{bcc}	β_{ccc}	β_{caa}	β_{cbb}	β_{μ}
monomer	1351	−43	−16	−184	505	4	1	−36	−7	799
dimer	1739	−61	−34	−2	−3	0	3	−60	−10	987
unit cell	3238	−117	−65	−73	171	3	5	−121	−23	1835

[a] The indices *a*−*c* refer to the axes of the crystal, while the numbers in parentheses refer to the MNA molecules (see also Figure 2). $\beta_{\mu} = 3/5(\beta_x\mu_x + \beta_y\mu_y + \beta_z\mu_z)/||\mu||$ with $\beta_i = \beta_{ixx} + \beta_{iyy} + \beta_{izz}$ and $||\mu||$ the norm of the dipole moment.

total energies of clusters containing two unit cells (i.e., eight MNA molecules) translated along the *c* axis. This value for the rotation angle agrees with the value adopted by Zyss and Oudar.[6]

IV. Results

Adopting the supramolecular approach, the bulk nonlinear susceptibility $\chi^{(2)}$ can, in principle, be determined by evaluating the first hyperpolarizability of increasingly large MNA clusters and then by extrapolating to infinite crystal size. This is the analogue of the oligomeric approach for polymers for which several extrapolation schemes have been designed.[38−40] For MNA, the clusters have been built by assembling (1,4) stacked dimers (see Figure 2 for the numbering of the MNA molecules) along each of the three crystal axes. The (1,4) stacked dimer appears effectively as the logical building block of the MNA crystal: its static electronic first hyperpolarizability tensor is dominated by the β_{aaa} component with the *a* crystallographic axis parallel to the C_2 axis of the dimer. As pointed out by Lipscomb et al.,[37] the *a* axis is almost parallel to the *X* principal axis. Table 1 lists the static electronic first hyperpolarizability tensor components in the crystal frame of the MNA stacked dimer as well as of its monomer and of the unit cell. With the exception of the monomer, the β_{aaa} component is at least 1 order of magnitude larger than the other tensor components. Similar to Hamada's evidence,[25] the formation of the dimer is accompanied by a large reduction of β_{aaa}/N. This reduction is also in agreement with the conclusions drawn in refs 17 and 18 for stacked dimers of *p*-nitroaniline.

(a) First Hyperpolarizabilities of "One-Dimensional" Molecular Clusters. For crystals, the computational effort is substantially larger than for polymers because the system spreads in all the spatial directions. Indeed, for a given saturation speed, N^3 unit cells have to be considered for a crystal whereas *N* units are sufficient for a polymer. Hopefully, the saturation in molecular crystals will be faster and, as demonstrated in paragraph IV.b, a simple multiplicative scheme will give access to the bulk nonlinear susceptibility. Contrary to diamond,[41] the unit cell size of the MNA crystal is large and simultaneous enlargement of the crystal in the three spatial directions goes rapidly beyond our computational resources. In a first step we have therefore investigated the evolution of the first hyperpolarizability in one-dimensional MNA clusters in order to address the long-range character of the crystal packing effects upon β_{aaa}. These MNA clusters have been built by aligning (1,4) stacked dimers in each crystal direction. For instance, the cluster with two stacked dimers aligned in the *a* direction contains the molecules 1, 4, 5, and 8 (see Figure 2). For the *b* directions, an even number of dimers has been considered because for odd numbers, there are substantial nondiagonal β components. Therefore, along this direction, the clusters are built by successive addition of unit cells (containing the molecules 1−4) rather than the addition of translated (1,4) stacked dimers. For instance, $N = 2$ means that the cluster built along the *b* direction corresponds to the unit cell A, while $N = 4$ stands for the unit cells A and C (see Figure 2). The AM1 β_{aaa} values are reported in Table 2 for increasingly large one-dimensional MNA-dimer chains as well as their crystal packing ratios. When the cluster is increased along the *a* axis, β_{aaa} per MNA dimer increases substantially whereas extending the cluster along the *b* and *c* axes leads to a decrease. Although the magnitude of these effects depends on the nature of the molecules, the qualitative trends are in agreement with simple electrostatics.[20−21] Indeed, the presence of a second molecule (II) along the field direction (corresponding to the situation where the cluster extends along the *a* axis) enhances the field amplitude on the reference site (I) as a consequence of the field-induced dipole moment on molecule II. At the opposite, when the molecules are aligned perpendicular to the field direction (corresponding to packing along the *b* and *c* axes), the induced dipole moment on II leads to a decrease of the field felt on site I. As shown by the numbers in Table 2, the corresponding ratios saturate with the size of the one-dimensional chain. By adopting the extrapolation procedures described in refs 38 and 39, the infinite chain length values of *R* have been calculated and are reported at the bottom of Table 2.

TABLE 2: AM1 β_{aaa} (in au) and Crystal Packing Ratios [$R_{(1,4)} = \beta^{cluster}/(N\beta^{(1,4)}) = R$] for Increasingly Large "One-Dimensional" Clusters[a]

no. of stacked dimers (*N*)	*a* axis		*b* axis		*c* axis	
	β_{aaa}	*R*	β_{aaa}	*R*	β_{aaa}	*R*
2	6336	1.822	3238	0.931	2559	0.736
3	13616	2.610			3380	0.648
4	22407	3.221	5663	0.814	4181	0.601
5	32072	3.689			4992	0.574
6	42212	4.046	8006	0.767	5801	0.556
7	52622	4.323			6606	0.543
8	63102	4.536	10345	0.744	7408	0.533
∞		5.1 ± 0.2		0.72 ± 0.01		0.51 ± 0.01

[a] The reference unit is the (1,4) stacked dimer (see Figure 2). The clusters extended along the *a* and *c* axes are built by successively adding dimers along these directions, respectively. For the *b* direction, the clusters contain an even number of dimers corresponding therefore to successive addition of unit cells containing four MNA molecules.

In a second step, a similar building strategy has been used for one-dimensional arrays of (1,2,3,4) unit cells along the *a* and *c* directions. The corresponding β_{aaa} and *R* values are listed in Table 3. The *R* values display the same behavior with the number of unit cells as the arrays of (1,4) stacked dimers. Indeed, for the *a* direction, $R > 1$ and increases with *N* whereas $R < 1$ and decreases with *N* when the clusters are enlarged in the *c* direction. Similarly, as far as it can be seen, these ratios tend to saturate with *N*. It is interesting to note that the $R_{(1,4)}$

TABLE 3: AM1 β_{aaa} (in au) and Crystal Packing Ratios [$R_{(1,4)} = \beta^{cluster}/N\beta^{(1,4)} = R$] for Increasingly Large "One-Dimensional" Clusters[a]

no. of unit cells (N/2)	a axis		c axis	
	β_{aaa}	R	β_{aaa}	R
2	10747	1.545	4568	0.657
3	23146	2.218	5836	0.559
4	39224	2.819	7107	0.511

[a] N stands for the number of stacked dimers. The building block is the (1,2,3,4) unit cell (see Figure 2) containing four MNA molecules.

ratios obtained for the arrays of (1,2,3,4) unit cells (see columns 3 and 5 of Table 3) can be, with a good accuracy, estimated by multiplying the corresponding $R_{(1,4)}$ ratios obtained for one-dimensional arrays of (1,4) stacked dimers (reported in Table 2). For instance, for four unit cells along the a axis $R_{(1,4)} = 2.819$ (Table 3) whereas the estimated ratio calculated from Table 2 is $3.221 \times 0.931 = 2.999$, where 3.221 (0.931) is the corresponding $R_{(1,4)}$ ratio for four (two) (1,4) stacked dimers aligned along the a (b) axis. We show in the next paragraph that the adequacy of this simple multiplicative scheme improves when considering interactions between complete unit cells.

(b) Hyperpolarizabilities of "Two-Dimensional" Molecular Clusters and Second-Order Susceptibility of MNA Crystal. In a third step, we have evaluated the β tensor components of molecular clusters extending in two crystal directions, i.e. a and b, a and c, and b and c. The largest clusters considered contain four unit cells (sixteen MNA molecules). The β_{aaa} tensor components and the $R = R_{(1,4)}$ values are given in Table 4 as well as the corresponding quantities for their subclusters made of two unit cells. For all combinations of two crystal directions, it has been found that the crystal packing ratio is, to within 2−3%, exactly reproduced by multiplying the ratios associated with the two corresponding crystalline directions. For example, the ratios for the clusters built from the A + B (a direction) and A + C (b direction) unit cells are 1.545 and 0.814, respectively, and their product amounts to 1.258, whereas the calculation on the (A + B + C + D) cluster which extends simultaneously over the a and b directions provides a value of 1.239. Further confirmation of the adequacy of this simple multiplicative scheme is given for clusters extending in the c direction. The multiplicative scheme appears therefore as an efficient approach to estimate macroscopic from microscopic NLO responses.

Consequently, by adopting the multiplicative scheme, the effective static electronic β_{aaa} of the MNA (1,4) stacked dimer in the crystal amounts to

$$\begin{aligned}\beta_{aaa}^{\text{eff}} &= \beta_{aaa}^{(1,4)} R_{(1,4)}^{a}(N\rightarrow\infty)\, R_{(1,4)}^{b}(N\rightarrow\infty)\, R_{(1,4)}^{c}(N\rightarrow\infty) \\ &= 1739 \times 5.1 \times 0.72 \times 0.51 \text{ au} \\ &= 1739 \times 1.87 \text{ au} \\ &= (32 \pm 2) \times 10^2 \text{ au} \end{aligned} \quad (3)$$

Therefore, for a unit cell volume of 722.4 Å^3, which corresponds to a weight density of 1.40 g/cm,[26,37]

$$\begin{aligned}\chi_{aaa}^{(2)} &= \beta_{aaa}^{\text{eff}}/(\epsilon_0 V^{\text{dimer}}) \\ &= 2\beta_{aaa}^{\text{eff}}/(\epsilon_0 V^{\text{unit cell}}) \\ &= 32.6 \text{ pm/V} \end{aligned} \quad (4)$$

(c) AM1 versus ab Initio First Hyperpolarizabilities of Monomer and Dimers. To assess the reliability of the semiempirical AM1 calculations, the static electronic first hyperpolarizabilities of the MNA molecule and of different dimers have been calculated with various ab initio schemes and are reported in Table 5. At the CPHF level, the variations in β_{aaa} with the basis set are consistent with previous investigations (see for instance ref 4); i.e., (i) β_{aaa} decreases when going from 6-31G to 6-31G** and (ii) adding diffuse P (6-31++G) or D (6-31G+D) functions increases β_{aaa}. With respect to the CPHF approach, the inclusion of electron correlation at the MP2 level leads to an increase of β_{aaa} by about 50% similar to the effect calculated by Sim et al.[42] for the longitudinal β tensor component of *p*-nitroaniline. The use of the AM1 Hamiltonian predicts a β_{aaa} value that is smaller than the correlated MP2/6-31G result but larger than all the CPHF ones. This indicates that, as in the case of γ of polyacetylene oligomers,[43] the AM1 parametrization implicitly includes a part of the electron correlation necessary to the description of nonlinear polarization effects of MNA.

Although these monomer β_{aaa} values cover a wide range (from 943 to 1702 au), all methods predict very similar crystal packing effects for various MNA dimers. In particular, the AM1 Hamiltonian reproduces to within 3% the R ratios determined at the MP2/6-31G level whereas the monomer AM1 β_{aaa} values differ by about 20%. Furthermore, changing the basis set has very little impact on these crystal packing ratios. On the basis of this dimer investigation it appears that the AM1 parametrization is a method of choice for determining the crystal packing effects on the first hyperpolarizability of MNA crystals: it provides the quality of ab initio correlated methods at a reduced computational price. In addition, since the semiempirical and ab initio methods adopted here provide very similar crystal packing ratios, improved crystal nonlinear susceptibility can be obtained by combining the AM1 crystal packing ratios with the ab initio correlated dimer first hyperpolarizability.

TABLE 4: AM1 β_{aaa} (in au) and Crystal Packing Ratios ($R_{(1,4)} = R$) for "Two-Dimensional" Clusters[a]

cluster	β_{aaa}	R	R estimated
A + B	10747	1.545	
A + C	5663	0.814	
A + (A + c)	4568	0.657	
A + B + C + D	17243	1.239	1.258 (+1.5%)
A + (A + c) + B + (B + c)	13734	0.987	1.015 (+2.8%)
A + (A + c) + C + (C + c)	7484	0.538	0.534 (−0.6%)

[a] The reference unit is the (1,4) stacked dimer and the labels A, B, (A + c), ... correspond to unit cells (see Figure 2). (A + c) refers to the unit cell obtained by translating unit cell A by one unit along the c axis. In the last column, the R factors calculated from the multiplication method are reported as well as, in parentheses, the difference in percent with respect to the value of the third column.

TABLE 5: First Hyperpolarizability Tensor Components (in au) for the MNA Molecule and Its Dimers Determined by the AM1 Semiempirical and by Various ab Initio Schemes[a]

	CPHF AM1	CPHF 6-31G	CPHF 6-31++G	CPHF 6-31G+D	CPHF 6-31G**	MP2 6-31G
$\beta_{aaa}^{\text{monomer}}$	1351	1112	1303	1201	943	1702
$R_{1,2}$	0.937	0.948	0.930	0.955	0.950	0.947
$R_{1,4}$	0.644	0.666	0.620	0.648	0.670	0.664
$R_{2,4}$	0.901	0.910	0.898	0.902	0.912	

[a] For the dimers the [$R = \beta^{\text{dimer}}/(2\beta^{\text{monomer}})$] ratios are provided. The frozen core approximation has been used in the MP2 calculations.

V. Further Discussions, Conclusions, and Outlook

The reported $\chi_{11}^{(2)}(-2\omega;\omega,\omega) \approx \chi_{aaa}^{(2)}(-2\omega;\omega,\omega)$ value is equal to 500 ± 150 pm/V at $\lambda = 1064$ nm ($\hbar\omega = 1.16$ eV).[37]

Accounting for the new quartz reference,[44] $\chi^{(2)}_{aaa}(-2\omega;\omega,\omega) = 300 \pm 75$ pm/V, which is 1 order of magnitude larger than our AM1 estimate for the static response. Since the crystal packing effect upon β has been shown to be almost independent of the method, $F_1 = \beta^{(1,4)}(\text{MP2})/\beta^{(1,4)}(\text{AM1}) = 1.3$ is a good correction factor for the missing electron correlation effects. Another correction can be made to account for frequency dispersion: $F_2(\omega) = \beta(-2\omega;\omega,\omega)/\beta(0;0,0)$. By using the two-state approximation for the monomer, $F_2(\omega) = \omega_{eg}{}^4/[\omega_{eg}{}^2 - 4\omega^2)(\omega_{eg}{}^2 - \omega^2)]$ with $\hbar\omega_{eg}$ the excitation energy of the dominant intramolecular charge-transfer excited state, a first estimate can be obtained. Taking the experimental $\hbar\omega_{eg} = 3$ eV value, $F_2(\omega) = 2.9$. Combining these two approximate corrections leads to a calculated $\chi^{(2)}_{aaa}(-2\omega;\omega,\omega) = \chi^{(2)}_{aaa}(0;0,0)[\text{AM1}]$ $F_1F_2(\omega) = 123$ pm/V that still underestimates the experimental data by 60%. This remaining large difference with respect to experiment can probably be attributed to the poor treatment of frequency dispersion, which lacks the intermolecular charge-transfer excitation effects.

In summary, we have proposed a simple multiplicative scheme to determine the macroscopic NLO response of molecular crystals from the knowledge of the NLO responses of small molecular clusters. We have illustrated the validity of this scheme for the static electronic second-order NLO response of the MNA crystal. We have also shown that the crystal packing effects upon the dominant β_{aaa} tensor component are different depending upon the crystal growth direction; resulting in an average 1.9 factor for β_{aaa} of the (1,4) stacked dimer. Using rough estimates for the frequency dispersion and the missing electron correlation effects, a calculated frequency-dependent second-order susceptibility of MNA crystal has been estimated. Nevertheless, the substantial difference with respect to the experimental value demonstrates the need to extend our approach toward explicit inclusion of frequency dispersion. In addition, it would be interesting to see whether an electrostatic model could yield closed-form expressions for the three *R* factors in eq 3 as a function of the crystal geometry. Further studies will also concentrate on assessing the validity of this scheme for other molecular crystals, cocrystals, or Langmuir−Blodgett films.

Acknowledgment. The authors thank O. Quinet for creating the MNA crystal structures and Pr. D. Liotard for helping them in running the AMPAC 6.0 program. F.C. thanks the Fondation Francqui for his postdoctoral fellowship. B.C. thanks the Belgian National Fund for Scientific Research for his Research Associate position. The calculations have been performed on the IBM and HP workstations of the Modelisation Pole of the Laboratoire de Physico-Chimie Moléculaire, as well as on the IBM SP2 of the Namur Scientific Computing Facility (Namur-SCF) for which the authors gratefully acknowledge the financial support of the FNRS-FRFC, the "Loterie Nationale" for the convention No. 2.4519.97.

References and Notes

(1) Kanis, D. R.; Ratner, M. A.; Marks, T. J. *Chem. Rev.* **1994**, *94*, 195.
(2) Brédas, J. L.; Adant, C.; Tackx, P.; Persoons, A.; Pierce, B. M. *Chem. Rev.* **1994**, *94*, 243.
(3) Kirtman, B.; Champagne, B. *Int. Rev. Phys. Chem.* **1997**, *16*, 389.
(4) Champagne, B.; Kirtman, B. In *Nonlinear Optical Materials*; Nalwa, H. S., Ed.; Handbook of Advanced Electronic and Photonic Materials and Devices, Vol. 9; Academic Press: New York, 2001; Chapter 2, p 63.
(5) Chemla, D. S.; Oudar, J. L.; Jerphagnon, J. *Phys. Rev. B* **1975**, *12*, 4534.
(6) Zyss, J.; Oudar, J. L. *Phys. Rev. A* **1982**, *26*, 2028.
(7) Zyss, J.; Berthier, G. *J. Chem. Phys.* **1982**, *77*, 3635.
(8) Tomasi, J.; Persico, M. *Chem. Rev.* **1994**, *94*, 2027.
(9) Amovilli, C.; Barone, V.; Cammi, R.; Cancès, E.; Cossi, M.; Menucci, B.; Pomelli, C. S.; Tomasi, J. *Adv. Quantum Chem.* **1999**, *32*, 227.
(10) Champagne, B.; Mennucci, B.; Cossi, M.; Cammi, R.; Tomasi, J. *Chem. Phys.* **1998**, *238*, 153.
(11) Cammi, R.; Mennucci, B.; Tomasi, J. J. *Am. Chem. Soc.* **1998**, *120*, 8834.
(12) Luo, Y.; Norman, P.; Ågren, H. *J. Am. Chem. Soc.* **1998**, *120*, 1188.
(13) Larsson, P. E.; Kristensen, L. M.; Mikkelsen, K. V. *Int. J. Quantum Chem.* **1999**, *75*, 449.
(14) Champagne, B.; Jacquemin, D.; André, J. M. In *Nonlinear Optical Properties of Organic Materials VIII*; Möhlmann, G. R., Ed.; SPIE Proceedings; SPIE: Bellingham, WA, 1995; No. 2527, p 71.
(15) Otto, P.; Gu, F. L.; Ladik, J. *J. Chem. Phys.* **1999**, *110*, 2717.
(16) Kirtman, B.; Gu, F. L.; Bishop, D. M. *J. Chem. Phys.* **2000**, *113*, 1294.
(17) Yasukawa, T.; Kimura, T.; Uda, M. *Chem. Phys. Lett.* **1990**, *169*, 259.
(18) Di Bella, S.; Ratner, M. A.; Marks, T. J. *J. Am. Chem. Soc.* **1992**, *114*, 5849.
(19) Dewar, M. J. S.; Zoebisch, E. G.; Healy, E. F.; Stewart, J. J. P. *J. Am. Chem. Soc.* **1985**, *107*, 3902.
(20) Dykstra, C. E. *J. Comput. Chem.* **1988**, *9*, 476.
(21) van Duijnen, P. Th.; de Vries, A. H. *Int. J. Quantum Chem.* **1995**, **S29**, 523.
(22) Munn, R. W. *Mol. Phys.* **1996**, *89*, 555.
(23) Kirtman, B.; Dykstra, C. E.; Champagne, B. *Chem. Phys. Lett.* **1999**, *305*, 132.
(24) Reis, H.; Papadopoulos, M. G.; Hättig, C.; Angyan, J. G.; Munn, R. W. *J. Chem. Phys.* **2000**, *112*, 6161.
(25) Hamada, T. *J. Phys. Chem.* **1996**, *100*, 8777.
(26) Hamada, T. *J. Phys. Chem.* **1996**, *100*, 19344.
(27) Cohen, H. D.; Roothaan, C. C. J. *J. Chem. Phys.* **1965**, **43**, S34.
(28) AMPAC 6.0; Semichem, 7204 Mullen, Shawnee, KS 66216, 1997.
(29) Kurtz, H. A.; Stewart, J. J. P.; Dieter, K. M. *J. Comput. Chem.* **1990**, *11*, 82.
(30) See for instance: Langhoff, P. W.; Karplus, M.; Hurst, R. P. *J. Chem. Phys.* **1966**, *44*, 505. Caves, T. C.; Karplus, M. *J. Chem. Phys.* **1969**, *50*, 3649. Dykstra, C. E.; Jasien, P. G. *Chem. Phys. Lett.* **1984**, *109*, 388.
(31) Frisch, M. J.; Trucks, G. W.; Schlegel, H. B.; Scuseria, G. E.; Robb, M. A.; Cheeseman, J. R.; Zakrzewski, V. G.; Montgomery, J. A., Jr.; Stratmann, R. E.; Burant, J. C.; Dapprich, S.; Millam, J. M.; Daniels, A. D.; Kudin, K. N.; Strain, M. C.; Farkas, O.; Tomasi, J.; Barone, V.; Cossi, M.; Cammi, R.; Mennucci, B.; Pomelli, C.; Adamo, C.; Clifford, S.; Ochterski, J.; Petersson, G. A.; Ayala, P. Y.; Cui, Q.; Morokuma, K.; Malick, D. K.; Rabuck, A. D.; Raghavachari, K.; Foresman, J. B.; Cioslowski, J.; Ortiz, J. V.; Baboul, A. G.; Stefanov, B. B.; Liu, G.; Liashenko, A.; Piskorz, P.; Komaromi, I.; Gomperts, R.; Martin, R. L.; Fox, D. J.; Keith, T.; Al-Laham, M. A.; Peng, C. Y.; Nanayakkara, A.; Gonzalez, C.; Challacombe, M.; Gill, P. M. W.; Johnson, B.; Chen, W.; Wong, M. W.; Andres, J. L.; Gonzalez, C.; Head-Gordon, M.; Replogle, E. S.; Pople, J. A. *Gaussian 98*, Revision A.7; Gaussian, Inc.: Pittsburgh, PA, 1998.
(32) Hehre, W. J.; Ditchfield, R.; Pople, J. A. *J. Chem. Phys.* **1972**, *56*, 2257.
(33) Hariharan, P. C.; Pople, J. A. *Theor. Chim. Acta* **1973**, *28*, 213.
(34) Hehre, W. J.; Ditchfield, R.; Pople, J. A. *J. Chem. Phys.* **1972**, *56*, 2257.
(35) Hurst, G. J. B.; Dupuis, M.; Clementi, E. *J. Chem. Phys.* **1988**, *89*, 385. Perez, J.; Dupuis, M. *J. Phys. Chem.* **1991**, *95*, 6525. Only the diffuse *D* functions have been considered. Their exponents have been fixed at 0.05, 0.07, and 0.10 for carbon, nitrogen, and oxygen atoms, respectively.
(36) Davis, P. J.; Rabinowitz, P. *Numerical Integration*; Blaisdell Publishing Co.; London, 1967; p 166. And, for an example: Jacquemin, D.; Champagne, B.; André, J. M. *Int. J. Quantum Chem.* **1997**, *65*, 679.
(37) Lipscomb, G. F.; Garito, A. F.; Narang, R. S. *J. Chem. Phys.* **1981**, *75*, 1509.
(38) Kirtman, B.; Toto, J. L.; Robins, K. A.; Hasan, M. *J. Chem. Phys.* **1995**, *102*, 5350.
(39) Champagne, B.; Jacquemin, D.; André, J. M.; Kirtman, B. *J. Chem. Phys. A* **1997**, *101*, 3158.
(40) Weniger, E. J.; Kirtman, B. Computers and Mathematics with Applications. Submitted for publication.
(41) Bishop, D. M.; Gu, F. L. *Chem. Phys. Lett.* **2000**, *317*, 322.
(42) Sim, F.; Chin, S.; Dupuis, M.; Rice, J. E. *J. Phys. Chem.* **1993**, *97*, 1158.
(43) See Table XX of ref 4.
(44) Roberts, D. A. *IEEE J. Quantum Elect. QE* **1992**, *28*, 2057. Mito, A.; Hagimoto, K.; Takahashi, C. *Nonlinear Opt.* **1995**, *13*, 3.